Effect of rare-earth doping in RCrSb$_3$ (R=La, Pr, Sm, and Gd)

D. D. Jackson
Lawrence Livermore National Laboratory, Livermore, California 94550, USA

Z. Fisk
Department of Physics, University of California, Davis, California 95616, USA

(Received 8 November 2005; revised manuscript received 12 December 2005; published 25 January 2006)

We report on the electrical resistivity and magnetic susceptibility of La or Gd doped RCrSb$_3$ (R=La, Pr, Sm, and Gd). Single crystals were grown by increasing the nominal dopant by 25%. In general, two magnetic ordering transitions are found, T_{c1} is attributed to ferromagnetic ordering of the itinerant Cr sublattice, and, at lower temperatures, T_{c2} is attributed to ordering of the localized rare-earth sublattice. Alloying on the rare-earth site varies the de Gennes factor, DG$=(g-1)^2J(J+1)$, and dT_{c1}/d(DG)$=-2$ K, while dT_{c2}/d(DG)$=5$ K. These ordering temperatures are found to converge at GdCrSb$_3$, where a single ferrimagnetic transition is found at $T_{c2}=86$ K due to an antialignment of the itinerant Cr magnetic sublattice and the localized rare-earth magnetic sublattice. Initially, for DG<3.5, the two magnetic sublattices order in a ferromagnetic ground state, and the paramagnetic Weiss temperature decreases at the same rate as T_{c1}. But for DG>4.5, the rare-earth magnetic sublattice antialigns with respect to the Cr sublattice, and the Weiss temperature decreases five times as fast. In the region between ($3.5<$DG<4.5), a first-order phase transition is found at T_{c2}.

DOI: 10.1103/PhysRevB.73.024421 PACS number(s): 75.30.Gw, 72.15.−v, 75.30.Cr

I. INTRODUCTION

The ternary compounds RCrSb$_3$ (R=La-Nd, Sm, Gd-Dy,Yb) have been studied extensively due to a number of their interesting physical properties. Among these are their quasiplanar crystal structure within the b-c plane as seen in Fig. 1(a),[1] the anomalous magnetism found in LaCrSb$_3$,[2–6] and the complex interaction between the itinerant 3d electrons from the Cr ions and the localized 4f moments from the rare-earth ions.[7–13] The parent member in the series, LaCrSb$_3$, has been studied in depth[2–4] because it has only one magnetic ion, Cr, yet it has a complex magnetic phase diagram including a ferromagnetic (FM) transition at $T_{c1}=132$ K, followed by a spin reorientation phase for $T<98$ K and $H<250$ G. The members R=Ce-Nd, and Sm show a second magnetic ordering at lower temperatures ($T_{c2}=10$–30 K) due to the alignment of the rare-earth ions.[7–12] The rare-earth ordering is ferromagnetic for R=Ce, Pr, and Nd, but antiferromagnetic (AFM) and first order for R=Sm. Polycrystalline samples of R=Gd, Tb, and Dy show only one magnetic transition.[8,11] Single crystals of GdCrSb$_3$ indicate this is a ferrimagnetic transition at $T_{c2}=86$ K due to antialignment of the Cr sublattice and the Gd^{3+} sublattice.[13] Recently, the series has been extended out to YbCrSb$_3$, where a single FM transition was found at 280 K, the largest magnetic ordering temperature in this family of compounds.[14] This large value was believed to be due in part to the divalent Yb^{2+} ion.

In this study, we alloy with La or Gd because they can be thought of as being on opposite ends of the spectrum and act as a convenient way to investigate the interactions between the localized rare-earth 4f moments and the itinerant Cr 3d electrons. The unit-cell volume is largest for LaCrSb$_3$ and decreases due to the lanthanide contraction going to GdCrSb$_3$. While they both have only one magnetic ordering temperature, the type of ordering is different for the two, and all the compounds in between have two distinct magnetically ordered phases. By doping on the rare-earth site, we can vary the number of 4f electrons which provides a means to investigate the behavior of the second magnetic ordering temperature.

We investigate La$_{1-x}$Gd$_x$CrSb$_3$ as a way to observe the transition from one end of the series to another, and track the evolution of the second-ordering temperature from $T_{c2}=0$ K for LaCrSb$_3$ to $T_{c2}=86$ K for GdCrSb$_3$. The first-order AFM transition found in SmCrSb$_3$ at $T_{c2}=30$ K has been investigated in detail elsewhere (see Ref. 12) and is unique to this family of compounds, which makes it a great candidate to study. PrCrSb$_3$ was chosen because it has very similar properties with NdCrSb$_3$,[7–9] which has been investigated in detail by neutron-diffraction measurements[10] showing that the Cr sublattice orders along the b axis at $T_{c1}=108$ K, and the second transition at $T_{c2}=13$ K is due to FM alignment of both the Cr and the Nd^{3+} lattices along the a axis, the stacking direction. By doping these compounds with La^{3+} (removing 4f electrons), one can track the disappearance of the rare-earth ordering. On the other hand, the development of the ferrimagnetic phase can be followed by doping with Gd^{3+} (increasing 4f electrons).

II. EXPERIMENTAL TECHNIQUE

The procedure for growing single crystals of RCrSb$_3$ has been previously described.[3] These samples crystallize in an orthorhombic structure (space group $Pbcm$),[1] and consist of two distinct planar layers of Cr and Sb perpendicular to the a axis, which are separated by the rare-earth ions (Fig. 1). The first of these layers consist of chains of Cr atoms extending along the c direction, with Sb atoms forming face sharing (edge sharing) octahedra along the c axis (b axis). The rare-

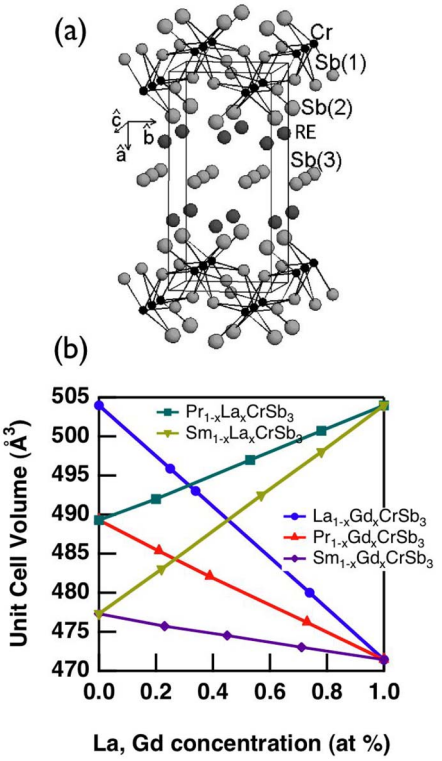

FIG. 1. (Color online) (a) The crystal stucture of RCrSb$_3$ (from Ref. 4). The chains with face-sharing Cr octahedra run along the c axis, and the quasi-two-dimensional plane lie perpendicular to the a axis. (b) The room-temperature unit-cell volume of the alloys in the current investigation.

earth ions lie in a checkerboard-type pattern which alternates above and below the Sb plane. Due to this quasi-two-dimensional crystal structure, anisotropy plays a crucial role in understanding its properties. The lattice parameters were determined at room temperature using a commercial Scintag x-ray diffractometer using a Si standard, and a least-squares fit to a minimum of 20 peaks. Each alloy was grown by increasing the nominal dopant concentration by 25%, and Vegard's law was then used to determine the actual dopant concentration from the unit-cell volume. The resulting crystals were rectangular planes with a thin face parallel to the a axis, and the longest side parallel to the c axis. The lattice constants for the materials investigated here are shown in Fig. 1(b).

Magnetization and magnetic susceptibility measurements were taken with a commercial superconducting quantum interference device (SQUID) magnetometer (Quantum Design MPMSR2) in the temperature range 2–350 K and the magnetic field aligned along each of the three principle axes. All samples were field cooled. Electrical resistivity measurements were performed using a standard four-probe technique in the temperature range 5–295 K. All measurements were collected on as grown samples. The electrical resistivity of SmCrSb$_3$ was investigated under pressure up to 8 kbar using a nonmagnetic Be-Cu pressure clamp and flourinert as a pressure medium. The pressure was determined by the load applied to the pressure clamp at room temperature.

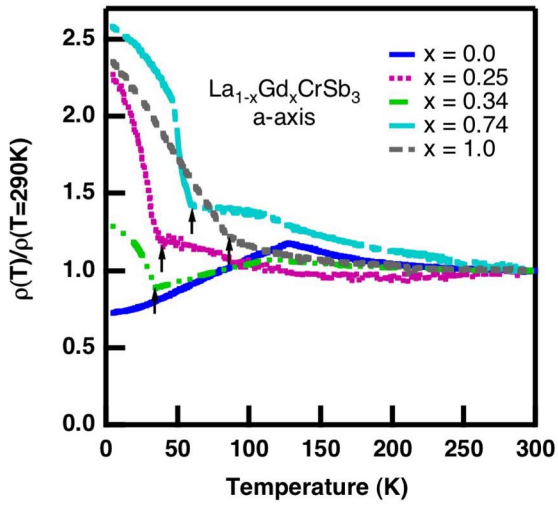

FIG. 2. (Color online) Normalized resistance vs temperature along the a axis for $La_{1-x}Gd_xCrSb_3$. The arrows point to the rare-earth ordering temperature T_{c2}.

III. RESULTS

We will begin with a discussion of $La_{1-x}Gd_xCrSb_3$, because it goes directly between the endpoints in the series. Figure 2 shows the normalized electrical resistivity as a function of temperature along the a axis (out-of-plane). For LaCrSb$_3$, the slope changes sign at $T_{c1}=132$ K.[3] With the addition of Gd^{3+}, a striking upturn is observed at the rare-earth ordering temperature. This sudden increase in the electrical resistivity increases in temperature and merges with the higher temperature FM ordered phase at GdCrSb$_3$.

Figure 3 shows the magnetization vs temperature along the c axis (in-plane) of $La_{1-x}Gd_xCrSb_3$ with an applied field of 1 kG. Despite the fact that Gd^{3+} has a half full $4f$-electron shell ($\mu_{eff}=7\mu_B$), and La^{3+} has no $4f$ electrons, we find that,

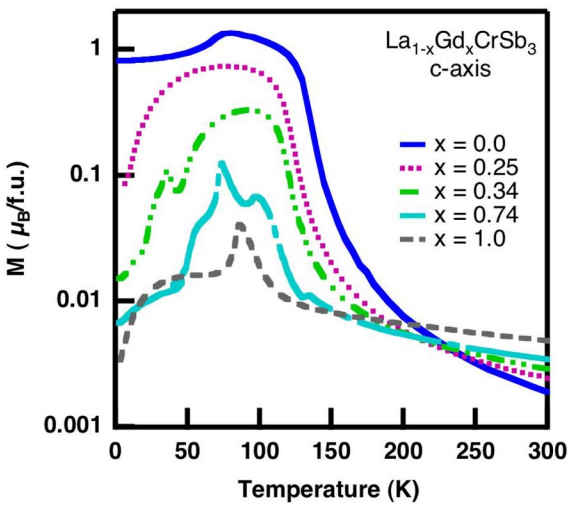

FIG. 3. (Color online) Magnetization vs temperature along the c axis for $La_{1-x}Gd_xCrSb_3$ with an applied field of 1 kG. The data are shown on a semilog plot in order for the magnetization transition to be seen for each alloy.

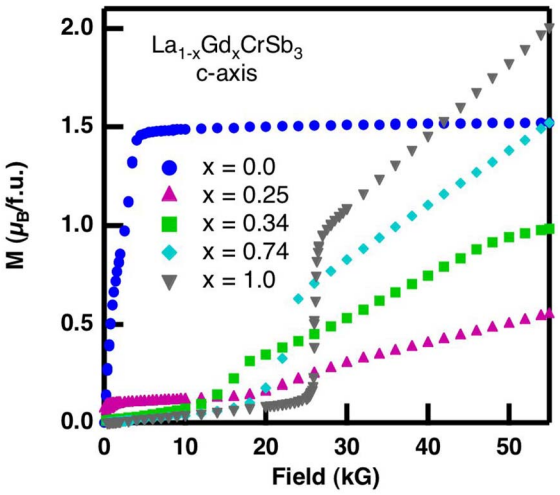

FIG. 4. (Color online) Magnetization vs field along the c axis for $La_{1-x}Gd_xCrSb_3$ at 5 K.

due to the disappearance of the FM ground state, increasing the concentration of Gd^{3+} actually reduces the magnetization. Furthermore, the increase in magnetization at T_{c1} shifts to lower temperatures with increasing Gd^{3+}. $LaCrSb_3$ has a shift in the magnetic easy axis from an alignment in the direction of the magnetic field within the plane immediately below T_{c1}, to alignment along the b axis as the temperature is reduced. A result of this is the drop in the magnetization below 75 K with an applied field of 1 kG. The drop at this point seen in Fig. 3 is therefore not due to a second magnetic ordering transition, but just realignment of the easy axis. On the other hand, the peak found for x=0.34, 0.74, and 1.0 does pinpoint the location of T_{c2}. No such peak is seen for x=0.25, which may be due to the dominating presence of the Cr ferromagnetism at this low concentration of Gd^{3+}.

The magnetization along the c axis at 5 K for $La_{1-x}Gd_xCrSb_3$ is shown in Fig. 4. First, as expected for a FM ground state, the magnetization for $LaCrSb_3$ very quickly saturates. For 25% Gd, the magnetization initially jumps up slightly, then remains constant for nearly 20 kG, followed by a linear increase with higher fields. As the Gd^{3+} concentration increases further, a met-magnetic transition develops and for $GdCrSb_3$, a sharp spin-flop transition is found at 25 kG. Recall that the magnitude of $M(T)$ steadily decreases with increasing Gd^{3+}. This surprising observation can be reconciled with the $M(H)$ results because none of the alloys with Gd^{3+} are ever found to saturate up to 55 kG, which is due to the ground state no longer being FM.

The series of alloys $La_{1-x}Gd_xCrSb_3$ show that the only one to have an itinerant FM ground state is $LaCrSb_3$. By adding Gd^{3+}, a second magnetic ordering temperature is present, T_{c2}, which is located by a kink in the electrical resistivity and a peak in the magnetization. Finally, the magnetization at a constant field dramatically decreases due to the non-FM ground state with the addition of Gd^{3+}.

$SmCrSb_3$ is unique in the family of compounds because it is found to have a strong first-order phase transition at T_{c2}=30 K (Fig. 5, and see Ref. 12 for a detailed review). By increasing the Gd^{3+} concentration, T_{c2} increases to higher

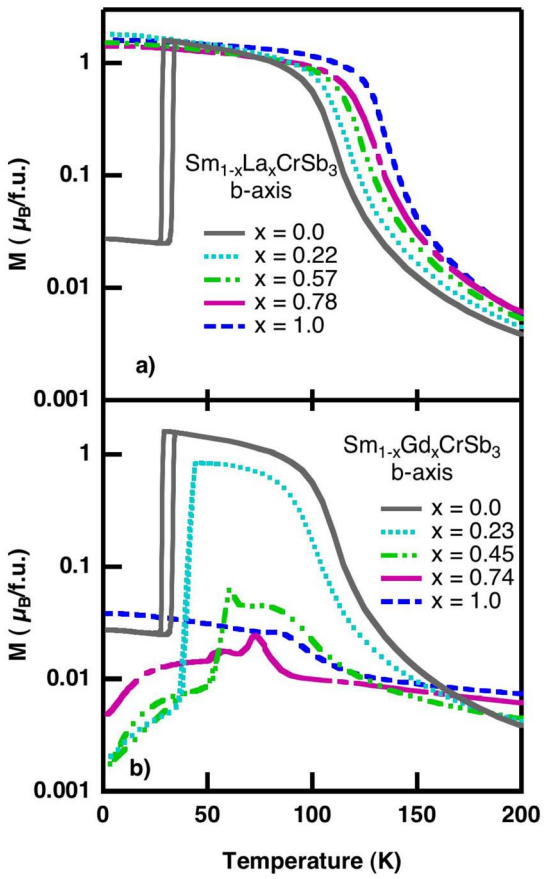

FIG. 5. (Color online) A semilog plot of the magnetization vs temperature along the b axis for (a) $Sm_{1-x}La_xCrSb_3$ and (b) $Sm_{1-y}Gd_yCrSb_3$ with an applied field of 1 kG. The hysteresis due to the first-order phase transition is located at $SmCrSb_3$ at T_{c2}=30 K.

temperatures [Fig. 5(b)]. While the transition is very sharp (~4 K wide) for $Sm_{0.77}Gd_{0.23}CrSb_3$, no hysteresis was found, and the transition does not appear to be first order. In addition, as was found for $La_{1-x}Gd_xCrSb_3$, the magnitude of the magnetization decreases with increasing Gd^{3+} concentration.

On the other hand, doping with La^{3+} quickly suppresses T_{c2}. With an applied field of 1 kG, Fig. 5(a) shows no evidence of a first-order transition for $x>0$. However, $Sm_{0.78}La_{0.22}CrSb_3$ has evidence for a first-order phase transition as found in $\rho(T)$ at zero field. The inset to Fig. 6(a) shows the electrical resistance along the a axis in which a jump in the resistance upon warming at T_{c2}=21 K is found. In addition, one of the properties of $SmCrSb_3$ below T_{c2} is that, along the b axis at 5 K, $M(H)$ has a large hysteresis loop which is entirely contained within the first quadrant. Figure 6(a) shows the magnetization along the b axis for $Sm_{1-x}La_xCrSb_3$, which shows that this off-center hysteresis loop persists for x=0.22. The rounded nature of this loop is most likely due to misalignment of the sample. Increasing the concentration of La^{3+} reduces the width of the hysteresis loop, and moves its position so that it is centered about zero field, as one would expect for a FM phase.

The first-order phase transition, which is only found in the pure compounds for $SmCrSb_3$, is fairly unstable with respect

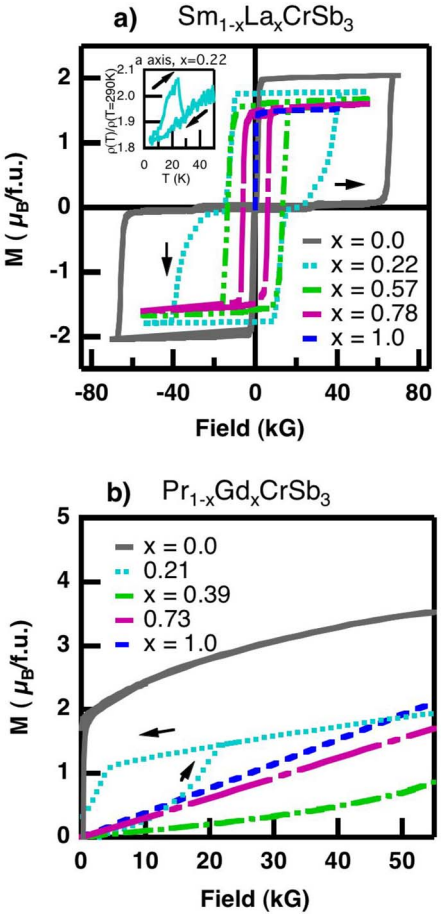

FIG. 6. (Color online) Magnetization vs field at 5 K along the b axis for (a) $Sm_{1-x}La_xCrSb_3$ and (b) $Pr_{1-x}Gd_xCrSb_3$. The inset to (a) shows the normalized electrical resistivity along the a axis for $Sm_{0.78}La_{0.22}CrSb_3$ with the $H=0$ hysteresis loop. The off-center hysteresis loop can be seen for $SmCrSb_3$, $Sm_{0.78}La_{0.22}CrSb_3$, and $Pr_{0.79}Gd_{0.21}CrSb_3$.

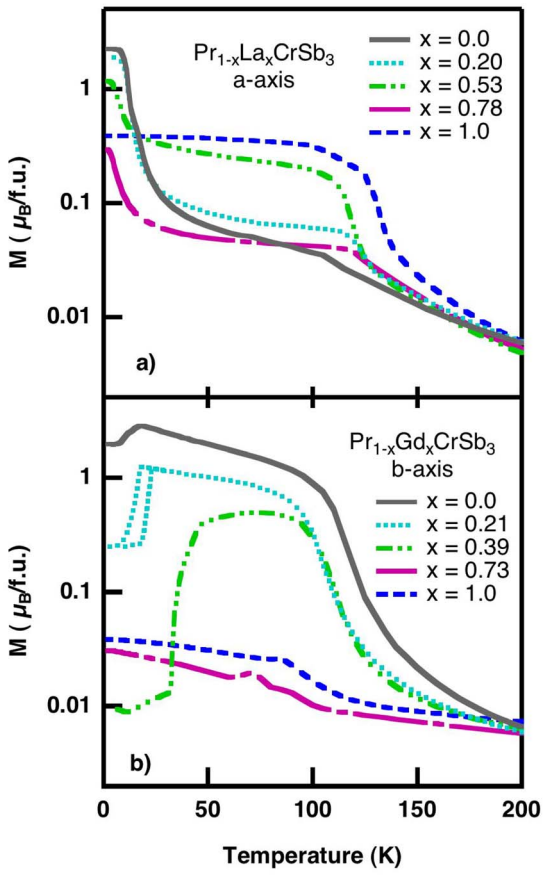

FIG. 7. (Color online) A semilog plot of the magnetization vs temperature for (a) $Pr_{1-x}La_xCrSb_3$ along the a axis, and (b) $Pr_{1-y}Gd_yCrSb_3$ along the b axis with an applied field of 1 kG. A first-order phase transition is found for $Pr_{0.79}Gd_{0.21}CrSb_3$ at $T_{c2}=16$ K.

to doping on the rare-earth site. While T_{c2} is still sharp with up to 45% Gd^{3+}, no hysteresis is observed, and the transition is no longer first order. The only alloy in which the transition continues to be first order is for 22% La^{3+}, which has hysteresis with zero magnetic field in the electrical resistivity. In addition, $Sm_{0.78}La_{0.22}CrSb_3$ shares the signature for this unique phase with an off-center magnetization vs field loop contained primarily in the first quadrant.

It has been shown by neutron-diffraction measurements that $NdCrSb_3$ orders ferromagnetically along the b axis due to the Cr electrons at $T_{c1}=108$ K, followed by a FM alignment of the Cr and Nd magnetic lattice at $T_{c2}=13$ K along the a axis.[10] In addition, both $PrCrSb_3$ and $NdCrSb_3$ have very similar magnetic and electrical transport properties,[7–9] and the magnetic anisotropy found for $PrCrSb_3$ is consistent with $NdCrSb_3$,[15] only the ordering temperatures are slightly different. For $PrCrSb_3$ the itinerant $3d$ electrons order at $T_{c1}=111$ K, followed by FM ordering of the localized $4f$ electrons at $T_{c2}=18$ K along the a axis. Figure 7(b) shows $M(T)$ along the b axis in which a strong increase at T_{c1} due to the Cr sublattice ordering with its easy axis along this direction, followed by a drop below T_{c2} due to a change in the direction of the easy axis accompanied with the FM ordering of the localized Pr^{3+} moments. A dramatic increase in the magnetization along the a axis at T_{c2} is due to the new easy axis being oriented in this out-of-plane direction.

Doping with La^{3+} removes $4f$ moments from the system, and the rare-earth ordering temperature monotonically decreases to zero [Fig. 7(a)]. The sharp increase in the magnetization below T_{c2} also decreases in magnitude. Conversely, doping with Gd^{3+} adds $4f$ electrons to the system, and T_{c2} increases to higher temperatures [Fig. 7(b)]. $Pr_{0.79}Gd_{0.21}CrSb_3$ shows the presence of a strong first-order phase transition at 16 K, with a hysteresis loop approximately 6 K wide which is similar to the transition found for $SmCrSb_3$. In addition, the unique off-center $M(H)$ hysteresis loop which is associated with this phase for $SmCrSb_3$ also appears for $Pr_{0.79}Gd_{0.21}CrSb_3$ [Fig. 6(b)]. Increasing the concentration of Gd^{3+} beyond 21% shows no evidence for a FM ground state.

$PrCrSb_3$ has two distinct magnetically ordered phases, but neither of these are associated with a first-order phase transition. However, $Pr_{0.79}Gd_{0.21}CrSb_3$ has a first-order phase transition at $T_{c2}=16$ K, which shares several properties with $SmCrSb_3$. Among these are the sharp drop in $M(T)$ along the b axis, and hysteresis in temperature, as well as in $M(H)$ in

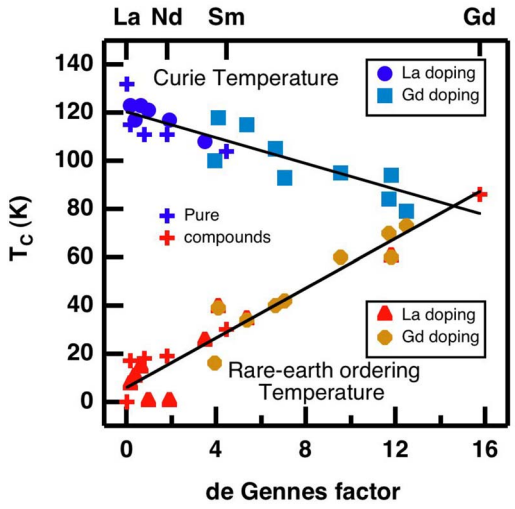

FIG. 8. (Color online) A plot of the Curie temperature and the rare-earth ordering temperature vs de Gennes factor for the pure compounds, RCrSb$_3$ (R=La-Nd, Sm, Gd), as well as the La and Gd doped samples investigated here. The top axis shows the location of the rare-earth elements associated with the de Gennes factor, plotted on the bottom axis.

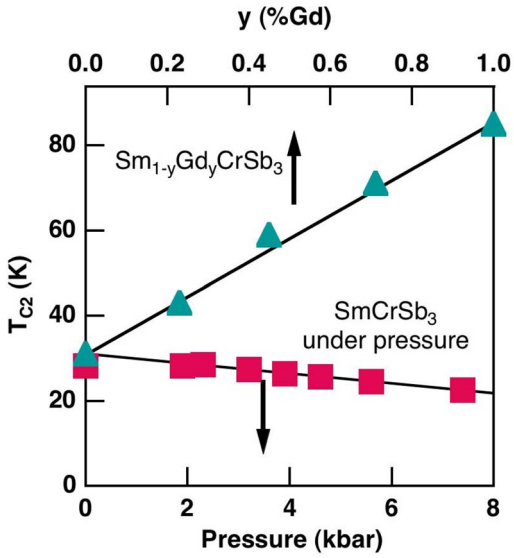

FIG. 9. (Color online) A comparison between the Néel temperature of $Sm_{1-x}Gd_xCrSb_3$ (triangles, top axis) and $SmCrSb_3$ under pressure (squares, bottom axis).

which the hysteresis loop is almost entirely contained within the first quadrant. Finally, the FM ground state is suppressed with Gd^{3+} doping, but persists for La^{3+} doping. Only in this case, the easy axis at 5 K changes from the a axis to the b axis (data not shown).

IV. DISCUSSION

The magnetism of rare-earth compounds is often described by the Ruderman-Kittel-Kasuya-Yosida (RKKY) interaction, in which the localized rare-earth moments interact through an indirect exchange via conduction electrons. The transition temperature θ within the Weiss molecular field theory, is related to the de Gennes factor, $\mathrm{DG}=(g-1)^2J(J+1)$, where g is the Landé g factor, and J is the total spin angular momentum, by[16]

$$\theta = 2\pi z A_0^2/k_B N(E_F)\mathrm{DG}\sum_{\mathbf{R}_i\neq\mathbf{R}_j}\phi(2k_F|\mathbf{R}_i-\mathbf{R}_j|), \qquad (1)$$

in which there are z conduction electrons per atomic volume, A_0 is the first-order coupling between the localized spins and the conduction electrons, $N(E_F)$ is the density of states at the Fermi level, k_F is the Fermi wave number, $\mathbf{R}_i$ is the lattice site of the ith localized spin, and $\phi(x)=[\sin(x)-x\cos(x)]/x^4$ is an oscillatory function due to the wave-number dependent susceptibility. Equation (1) shows that the magnetic ordering temperature should be linearly related to the de Gennes factor, and the type of ordering (FM or AFM) depends upon the oscillatory function, $\phi(x)$.

Figure 8 shows both T_{c1}, due to the itinerant Cr ions, and T_{c2}, due to the localized rare-earth ions, plotted verses the de Gennes factor. This figure combines all of the pure compounds, RCrSb$_3$ (R=La-Nd, Sm, Gd),[3,12,13,15] as well as the alloys investigated in this study. All of the rare-earth ordering temperatures linearly increase with the de Gennes factor at $dT_{c2}/d(\mathrm{DG})=5$ K, while the FM ordering due to the Cr ion decreases with de Gennes factor at a rate of $dT_{c1}/d(\mathrm{DG})=-2$ K. The two magnetic ordering phases converge to a single value at GdCrSb$_3$. This provides support to the conclusion that the single magnetic ordering temperature in GdCrSb$_3$ is a ferrimagnetic phase in which the itinerant $3d$ sublattice and the localized $4f$ sublattices are antialigned. The linear relationship between the rare-earth ordering temperature and de Gennes factor indicates that the interactions between the $4f$ moments are due to the RKKY interaction.

Alloying with Gd^{3+} not only varies the de Gennes factor by increasing the number of $4f$ electrons, but it also decreases the unit-cell volume due to lanthanide contraction. It is therefore useful to compare these results with that of applying physical pressure to the system. SmCrSb$_3$ has a large increase in the electrical resistivity along the a axis at the first-order phase transition.[12] It is therefore ideally suited to investigate the effects of pressure on the rare-earth ordering, and the results are shown in Fig. 9. It is immediately clear that Gd^{3+} doping has the opposite effect on T_{c2} from hydrostatic pressure on SmCrSb$_3$, illustrating that the volume change is not the primary cause for the increase in T_{c2}. On the other hand, using a simple band model, increasing pressure reduces the electronic density of states, which could account for the decrease in T_{c1}. The pressure measurements indicated that a trend toward $dT_{c1}/dP<0$, but the effect is subtle, and higher pressures will be required to confirm this behavior.

The moments at 55 kG and 5 K for the alloys are shown in Fig. 10. If the magnetization has saturated, this plot shows the value as a solid marker. The reason for the distinction is that several of the magnetization curves continue to increase at the maximum attainable field of 55 kG. The very low value of magnetization for $Pr_{0.61}Gd_{0.39}CrSb_3$(DG=6.63) along the b axis, for example, is due to this alloy being in a

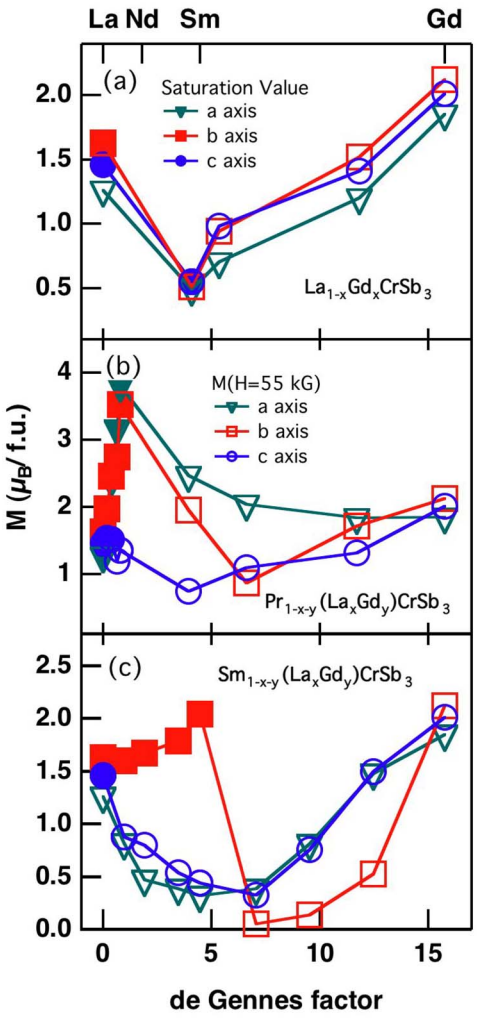

FIG. 10. (Color online) Magnetization at 5 K (saturated values represented by closed symbols) for the a axis (triangles), b axis (squares), and c axis (circles) for (a) $La_{1-x}Gd_xCrSb_3$, (b) $Pr_{1-x-y}(La_xGd_y)CrSb_3$, and (c) $Sm_{1-x-y}(La_xGd_y)CrSb_3$. Solid symbols represent the saturation value, and hollow symbols represent the value reached at 55 kG. The top axis shows the location of the rare-earth elements associated with the de Gennes factor, plotted on the bottom axis.

non-FM ground state [see Fig. 7(b)] in which the magnetization gradually increases with field [Fig. 6(b)]. The data generally indicate a minimum in the magnetization near DG$\simeq$4.5, and no axis has saturated by 55 kG for DG$>$5. All of the FM ground states are found for DG$<$4, and ferrimagnetic ground states for DG$>$4.5.

Initially, just below T_{c1}, the easy axis is within the b-c plane, and along the direction of the applied magnetic field. As the temperature is reduced further, the full magnetic anisotropy of the system becomes evident, and the easy axis becomes parallel to the b axis (see, for example, the drop in M_c for $LaCrSb_3$ in Fig. 3). While there is no universal behavior found for the development of the full magnetic anisotropy when doping on the rare-earth site, the temperature at which it develops tends to fall at a rate similar to the decrease in T_{c1} (data not shown).

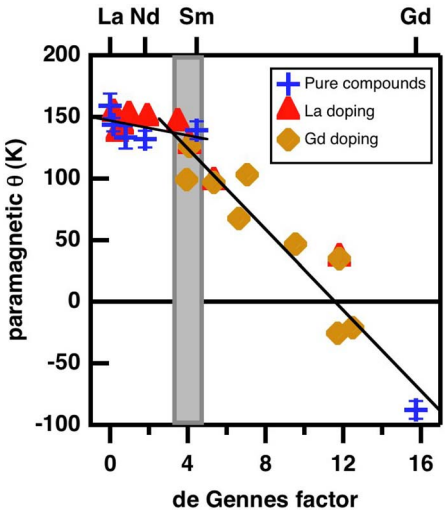

FIG. 11. (Color online) Value of θ obtained from the average of the three principle axes in the paramagnetic phase, $T>200$ K for the pure compounds (crosses), the La doped compounds (triangles), and Gd doped samples (diamonds). The shaded regions shows the region of the first-order AFM transition. The top axis shows the location of the rare-earth elements associated with the de Gennes factor, plotted on the bottom axis.

In the paramagnetic phase ($200\leqslant T\leqslant 350$ K), the magnetic susceptibility can be fit to a modified Curie-Weiss law, $\chi=C/(T-\theta)+\chi_0$, where C is the Curie constant and is related to the effective moment, θ is the paramagnetic Weiss temperature and indicates the strength and sign of the interaction, and χ_0 is a temperature-independent constant. The average value of the paramagnetic Weiss temperature, θ, obtained from the three principle axes for each alloy is shown in Fig. 11. It is clear that two distinct regions exist, centered near $SmCrSb_3$(DG$\sim$4.5). First, for DG$<$3.5 the Weiss temperature is positive, indicative of FM interactions, and falls at a slow rate of $d\theta/d(\mathrm{DG})=-3$ K. This is very close to the decrease found in the Curie temperature, $dT_{c1}/d(\mathrm{DG})=-2$ K, which shows that the ground state is dominated by the FM Cr sublattice. However, for DG$>$4.5, the Weiss temperature linearly decreases at a rate five times faster, $d\theta/d(\mathrm{DG})=-16$ K, and goes from positive (FM coupling) to negative (AFM coupling) values. In this region, the strength of the rare-earth coupling has a large effect on the ground state of the system, and the antialignment of the sublattices becomes increasingly dominant.

The shaded region near DG$\simeq$4 in Fig. 11 contains the results of four alloys, three of which exhibit a first-order phase transition to an AFM phase ($SmCrSb_3$, $Sm_{0.78}La_{0.22}CrSb_3$, and $Pr_{0.79}Gd_{0.21}CrSb_3$). While $La_{1-x}Gd_xCrSb_3$ did not have a first-order transition (DG $=4.1$, $x=0.25$ fell into this region but the transition at T_{c2} was not first order), this is likely due to the fact that Gd^{3+} has no orbital angular momentum, so that the magnetic anisotropy of this ion is greatly reduced. This shaded region is also the crossover from a FM ground state in which the localized rare-earth moments and the itinerant Cr sublattice align with the same easy axis for DG$<$3.5, and a ferrimagnetic ground state in which the rare-earth magnetic sublattice

and the Cr sublattice antialign with each other. Both Cr and Sb vacancies are known to exist in these family of compounds,[1,4,10] which appears to become more important as the rare-earth size decreases. YbCrSb_3 has also been shown to be the only member in which the rare-earth is divalent[14] due to electron transfer from the Cr-Sb octahedral to the Yb-Sb checkerboard plane. Similar changes in stoichiometry may transfer electrons from the valence band to bring about the change in coupling between the Cr and rare-earth sublattice. Further detailed investigations into the vacancies within the crystal structure will need to be carried out in order to investigate the substoichiometry of the compounds, both in detailed x-ray analysis, and by chemically varying the Cr and Sb content.

V. CONCLUSIONS

Alloying La^{3+} or Gd^{3+} into $R\mathrm{CrSb}_3$ for R =(La,Pr,Sm, or Gd) has the effect of varying the interactions between the localized $4f$ moments and the itinerant $3d$ moments so that the ground state of these materials varies from FM (R=La-Nd) to ferrimagnetic (R=Sm and Gd). The linear relationship found between the rare-earth ordering temperature and the de Gennes factor shows that the interaction between the $4f$ moments is due to the RKKY mechanism. The two magnetic ordering phases converge to a single ordering temperature for GdCrSb_3, suggesting that the ordering for this material is ferrimagnetic, in which the Cr sublattice antialigns with the localized rare-earth moments. The paramagnetic Weiss temperature, on the other hand, has a sharp kink near $\mathrm{DG}\simeq 4.5$ (SmCrSb_3), and the saturation value of the magnetization for the alloys has a minimum near this point. In addition, a first-order phase transition is found for SmCrSb_3 (DG=4.46), $\mathrm{Sm}_{0.78}\mathrm{La}_{0.22}\mathrm{CrSb}_3$ (DG=3.48), and $\mathrm{Pr}_{0.79}\mathrm{Gd}_{0.21}\mathrm{CrSb}_3$ (DG=3.94), which all lie near this kink. This suggests that the unique first-order phase transition found at 30 K for SmCrSb_3 is due to its location in this phase diagram where the coupling between the $3d$ and $4f$ moments change from FM to AFM. As the de Gennes factor continues to increase, AFM coupling between the magnetic sublattices becomes dominant and the Weiss temperature goes from an overall positive value to negative. Compounds with $\mathrm{DG}<3.5$ have an itinerant FM transition due to the Cr sublattice. The rare-earth moments also couple with FM interactions, which leads to a FM ground state. Therefore within this region, the Weiss temperature remains relatively constant and positive. While the Cr sublattice continues to undergo FM alignment for all the alloys across the series, the rare-earth moments begin to exhibit AFM coupling with the Cr sublattice for $\mathrm{DG}>4.5$. This causes the Weiss temperature to drop and eventually turn negative. GdCrSb_3 is therefore found to have a single ordering temperature in which the Cr magnetic sublattice is antialigned with the localized Gd^{3+} sublattice.

ACKNOWLEDGMENTS

Scott McCall and Mike Torelli have been helpful during many discerning discussions. We would also like to thank Julia Carmen for her insightful conversations. This work was funded in part by the In House Research Program at the National High Magnetic Field Laboratory, which was funded by the NSF, Cooperative Agreement No. DMR-9527035. This work was performed under the auspices of the U.S. Department of Energy by the University of California, Lawrence Livermore National Laboratory, under Contract No. W-7405-Eng-48.

[1] M. Brylak, W. Jeitschko, Z. Naturforsch., B: Chem. Sci. **B50** 899 (1995); M. Ferguson, R. Hushagen, and A. Mar, J. Alloys Compd. **249**, 191 (1997).
[2] N. P. Raju, J. E. Greedan, M. J. Ferguson, and A. Mar, Chem. Mater. **10**, 3630 (1998).
[3] D. D. Jackson, M. Torelli, and Z. Fisk, Phys. Rev. B **65**, 014421 (2002).
[4] E. Granado, H. Martinho, M. S. Sercheli, P. G. Pagliuso, D. D. Jackson, M. Torelli, J. W. Lynn, C. Rettori, Z. Fisk, and S. B. Oseroff, Phys. Rev. Lett. **89**, 107204 (2002).
[5] J. Shim and B. Min, J. Magn. Magn. Mater. **272-276**, e241 (2004).
[6] M. Richter, J. Rusz, H. Rosner, K. Koepernik, I. Opahle, U. Nitzsche, and H. Eschrig, J. Magn. Magn. Mater. **272-276**, e251 (2004).
[7] K. Hartjes, W. Jeitschko, and M. Brylak, J. Magn. Magn. Mater. **173**, 109 (1997).
[8] M. Leonard, S. Saha, and N. Ali, J. Appl. Phys. **85**, 4759 (1999).
[9] M. Leonard, I. Dubenko, and N. Ali, J. Alloys Compd. **303-304**, 265 (2000).
[10] L. Deakin, M. J. Ferguson, and A. Mar, Chem. Mater. **13**, 1407 (2001).
[11] L. Deakin and A. Mar, Chem. Mater. **15**, 3343 (2003).
[12] D. D. Jackson and Z. Fisk, J. Magn. Magn. Mater. **256**, 106 (2003).
[13] D. D. Jackson and Z. Fisk, J. Alloys Compd. **377**, 243 (2004).
[14] S. J. Crerar, L. Deakin, and A. Mar, Chem. Mater. **176**, 2780 (2005).
[15] D. D. Jackson and M. E. Torelli (unpublished); single crystals of CeCrSb_3 and NdCrSb_3 have also been investigated.
[16] K. N. R. Taylor and M. I. Darby, *Physics of Rare Earth Solids* (Chapman and Hall, Ltd., London, 1972).